SMAD4 promotes TGF-β-independent NK cell homeostasis and maturation and anti-tumor immunity

Youwei Wang[1,2,†], Jianhong Chu[2,†], Ping Yi[2,3,†], Wejuan Dong[2], Jennifer Saultz[2], Yufeng Wang[2], Hongwei Wang[2], Steven Scoville[2], Jianying Zhang[4], Lai-Chu Wu[2], Youcai Deng[2], Xiaoming He[5], Bethany Mundy-Bosse[2], Aharon G. Freud[2,6], Li-Shu Wang[7], Michael A. Caligiuri[8,*], Jianhua Yu[1,2,9,*]

Affiliations:
[1]Division of Hematology, Department of Internal Medicine, College of Medicine, The Ohio State University, Columbus, Ohio 43210, USA;
[2]The Ohio State University Comprehensive Cancer Center, Columbus, Ohio 43210, USA;
[3]Third Affiliated Hospital, Third Military Medical University, Chongqing 400038, China;
[4]Center for Biostatistics, The Ohio State University, Columbus, Ohio 43210, USA;
[5]Department of Biomedical Engineering, The Ohio State University, Columbus, Ohio 43210, USA;
[6]Department of Pathology, The Ohio State University, Columbus, Ohio 43210, USA;
[7]Division of Hematology and Oncology at the Medical College of Wisconsin, Milwaukee, WI 53226, USA;
[8]Department of Hematology, City of Hope National Medical Center, Duarte, CA 91010; USA
[9]The James Cancer Hospital, The Ohio State University, Columbus, Ohio 43210, USA

[†]These authors contributed equally to this work.

[*]Correspondence to: Jianhua Yu (jianhua.yu@osumc.edu). Biomedical Research Tower, Room 816, Department of Internal Medicine, Division of Hematology, The Ohio State University. 460 W 12th Ave, Columbus, OH 43210. Phone: 614-293-1471. Fax: 614-688-4028; Michael A. Caligiuri (mcaligiuri@coh.org), Department of Hematology, City of Hope National Medical Center, Duarte, CA 91010, Phone: 626-218-4328;

Keywords: SMAD4, Natural killer cells, Antitumor, NK cell development, GZMB, JUNB, Cytomegalovirus

Conflict of Interest: The authors declare no potential conflicts of interest.

Supplemental Material

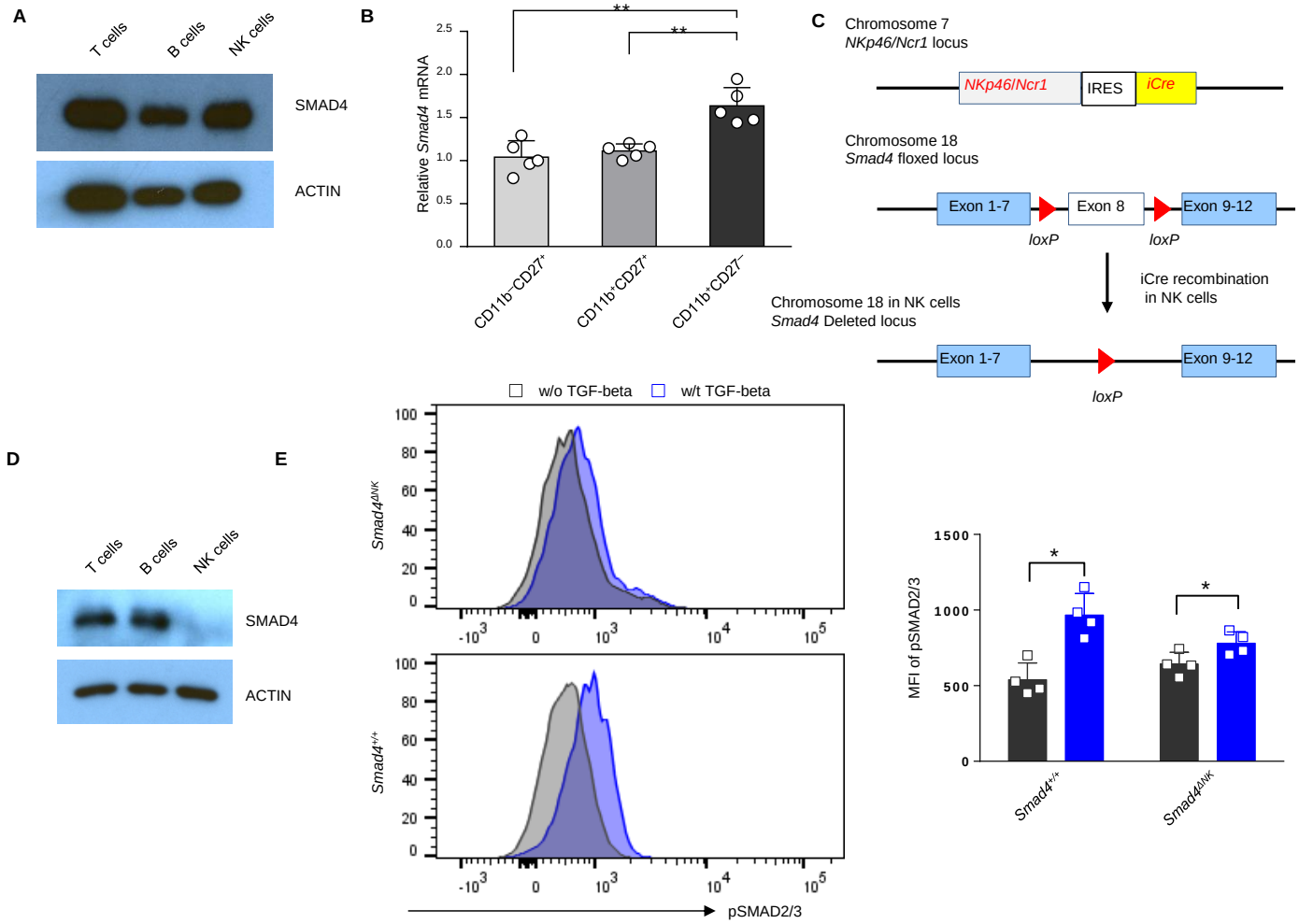

Supplemental Figure 1. Expression of *Smad4* in wild-type and conditional knock-out NK cells. (A) Expression of SMAD4 in T, B, and NK cells, determined by immunoblotting. (**B**) Expression of *Smad4* at each maturation stage of NK cells, determined by real-time RT-PCR (n = 5). ** $P < 0.01$, by one-way ANOVA and Holm's multiple comparisons test. The circles or squares on bar graphs denote data of individual mice. (**C**) Expression of *iCre* recombinase was under the control of the *NKp46* promoter. The exon 8 of *Smad4* gene, which was flanked by *LoxP* sites, was deleted in NK cells. (**D**) Immunoblotting was used to compare SMAD4 protein expression among T, B, and NK cells from *Smad4*$^{\Delta NK}$ mice. (**E**) The levels of pSMAD2/3 in wild-type and *Smad4*-deficient NK cells were assessed by intracellular flow cytometry with or without TGF-beta (10 ng/ml) stimulation for 30 min, (n = 4). Data were presented as mean ± SD. P values were calculated using two-tailed paired t test. ** $P < 0.01$. The squares on bar graphs denote data of individual mice.

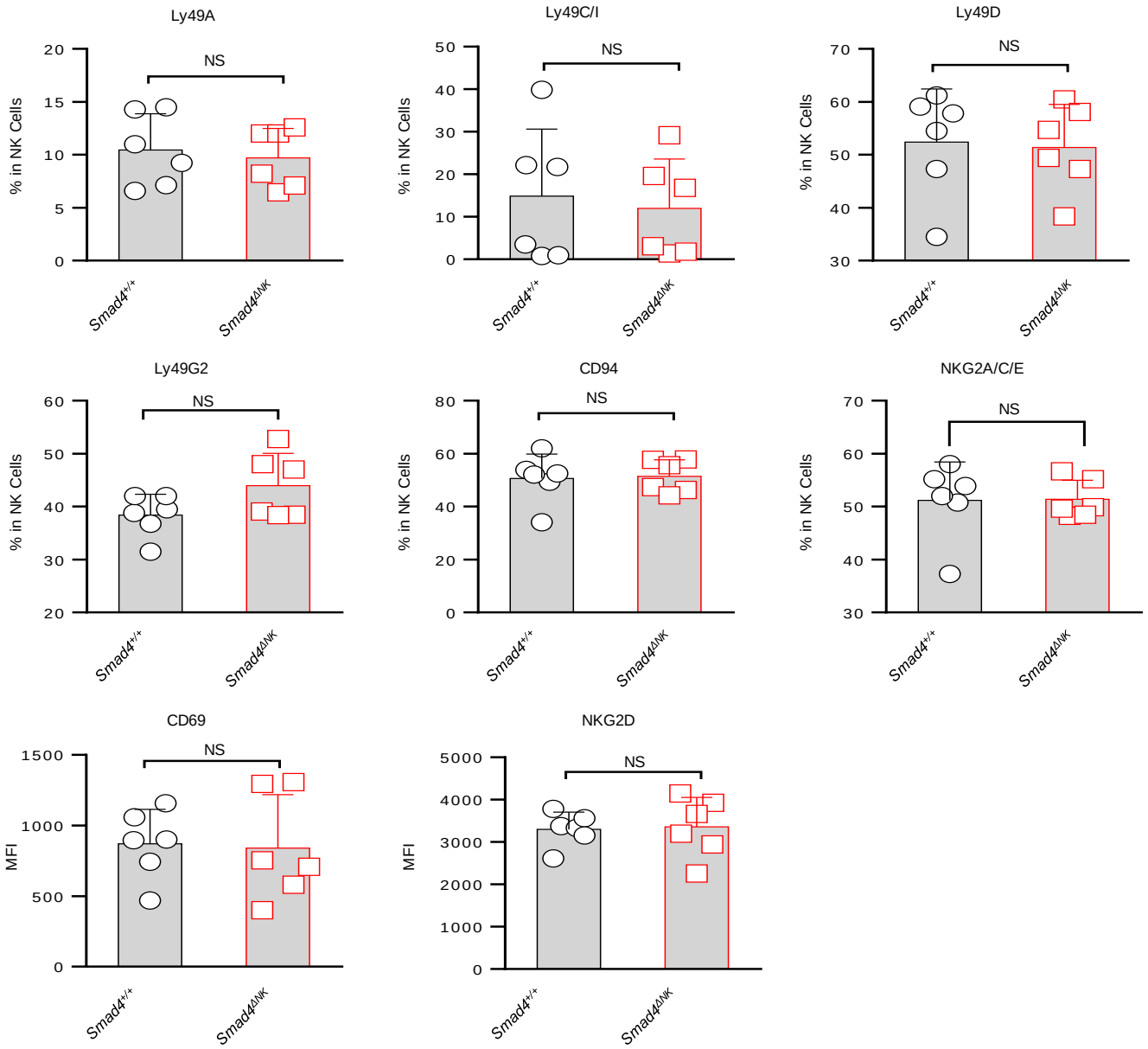

Supplemental Figure 2. Expression of inhibitory and activating receptors on NK cells from *Smad4*$^{+/+}$ and *Smad4*$^{\Delta NK}$ mice. The percentage of NK cells expressing cell surface markers Ly49A, Ly49C/I, Ly49G2, Ly49D, CD94, NKG2A/C/E, CD69, or NKG2D was determined by flow cytometry (n = 6). Data are presented as mean ± SD. Differences were evaluated between littermates. P values were calculated using two-tailed paired t test. NS, no significance. The circles or squares on bar graphs denote data of individual mice.

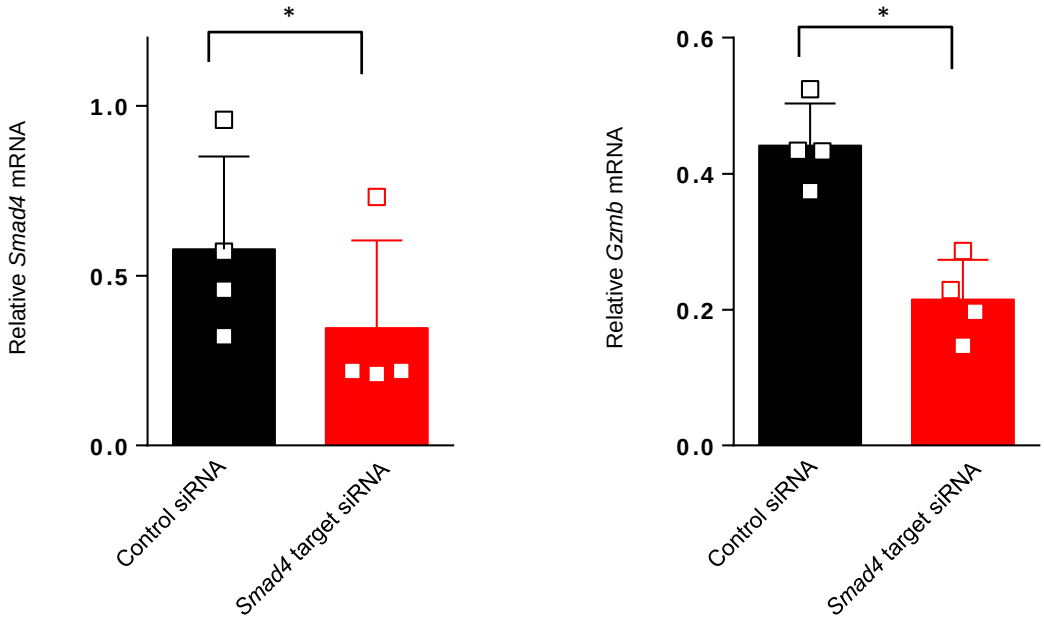

Supplemental Figure 3. siRNA-mediated knockdown of *Smad4* in NK cells. Negative control siRNA or *Smad4* target siRNA were transfected into enriched splenic NK cells isolated from spleens of C57BL/6 wild-type mice. Two days after transfection, the cells were harvested and the expression of *Smad4* and *Gzmb* was quantified by real-time RT-PCR. Data are represented as mean ± SD. *P* values were calculated using two-tailed paired *t* test. * $P < 0.05$.

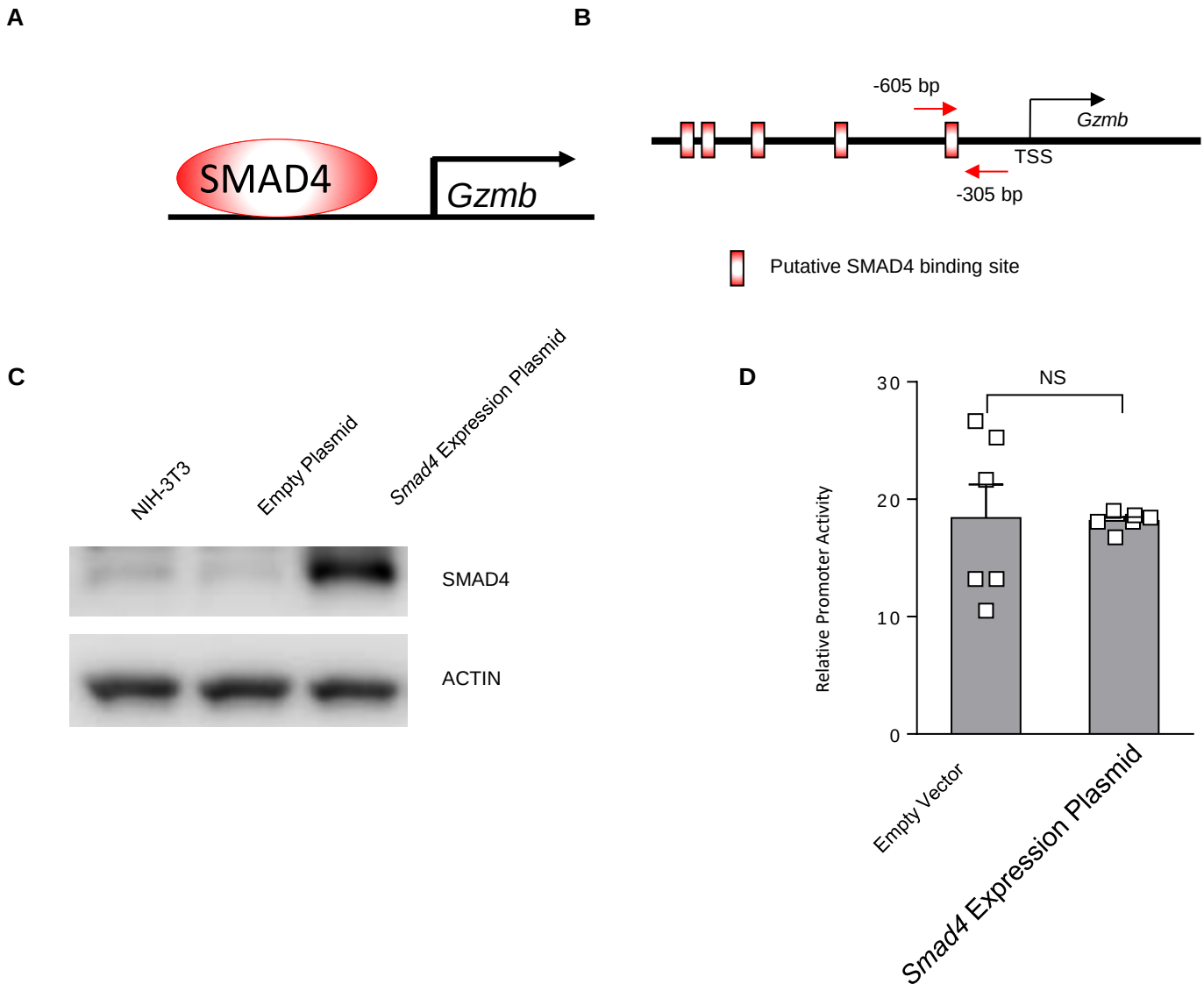

Supplemental Figure 4. SMAD4 transactivates the *Gzmb* promoter. (**A**) Potential mechanisms for regulation of *Gzmb* by SMAD4. (**B**) Putative SMAD4 binding sites in the *Gzmb* promoter. A scheme to denote five putative SMAD4 binding sites in the *Gzmb* promoter within 3 kb upstream of the transcription start site (TSS). (**C**) NIH-3T3 cells were transfected with a *Smad4* expression plasmid or an empty plasmid. Expression levels of SMAD4 and β-ACTIN were analyzed by immunoblotting. (**D**) A *Smad4* expression plasmid was co-transfected with a *Gzmb* promoter luciferase reporter plasmid as well as the pRL-TK control vector into NIH-3T3 cells. The levels of luciferase expression were analyzed 48 hr after transfection (n = 3). Data are presented as mean ± SD. P values were calculated using two-tailed t test. NS, no significance.

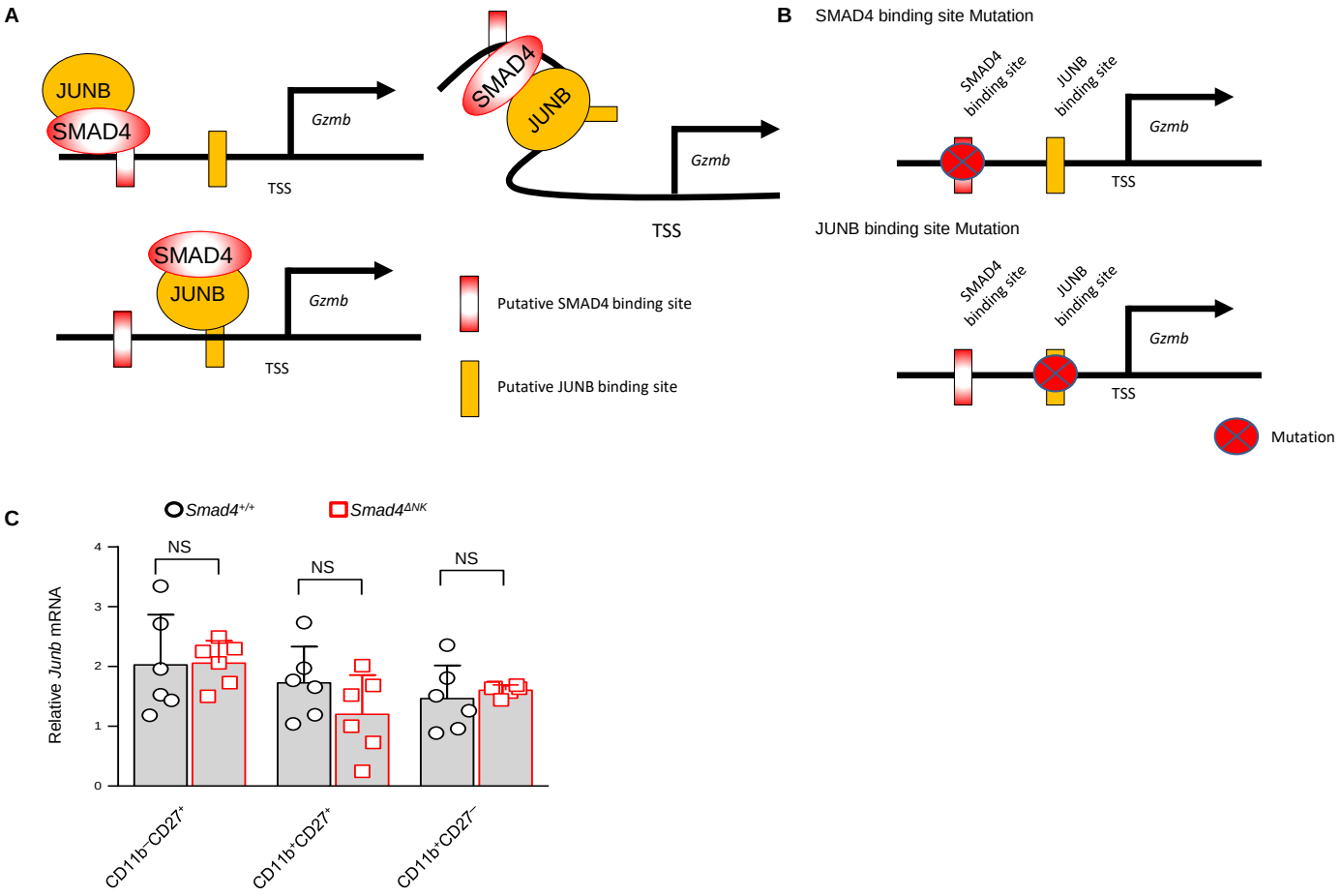

Supplemental Figure 5. SMAD4/JUNB complex binds to the JUNB binding site to transactivate the *Gzmb* promoter. (**A**) Potential mechanisms for transactivation of *Gzmb* by the SMAD4/JUNB complex. (**B**) Schemes denoting the mutation of the putative SMAD4 binding site or the putative JUNB binding site. The mutation was created using a QuikChange II Site-Directed Mutagenesis Kit. (**C**) Expression of *Junb* in NK cells at different stages of maturation was assessed by real-time RT-PCR (n = 6). The difference of *Junb* mRNA levels among different stages of maturation between *Smad4*-defficient and *Smad4*-sufficient NK cells is not statistically significant. Data are presented as mean ± SD. Differences were evaluated between littermates. P values were calculated using two-tailed paired t test. NS, not significant. The circles or squares on bar graphs denote data of individual mice.

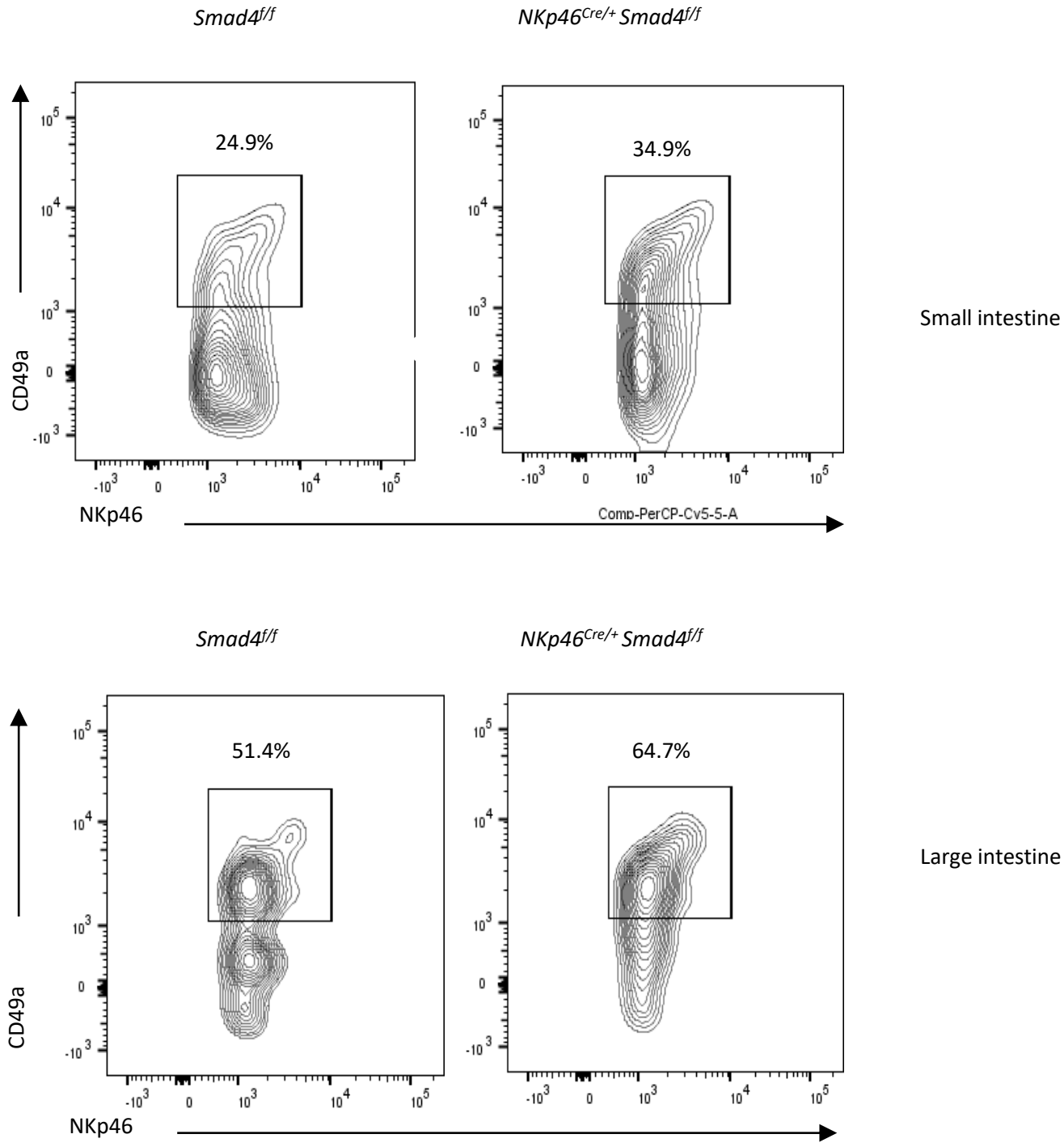

Supplementary Figure 6: The ILC1-like population is increased in the small and large intestines of *NKp46^{iCre}Smad4$^{fl/fl}$* mice. Cells were isolated from the small and large intestines of *Smad4*$^{fl/fl}$ and *NKp46^{iCre}Smad4*$^{fl/fl}$ mice and were subjected to a flow cytometric analysis. Cells were gated on CD3^{-}CD19^{-}NK1.1^{+} to assess NKp46 and CD49a expression. Numbers in quadrants indicate the percentage of ILC1-like cells. Data from one of five mice with similar data are presented.

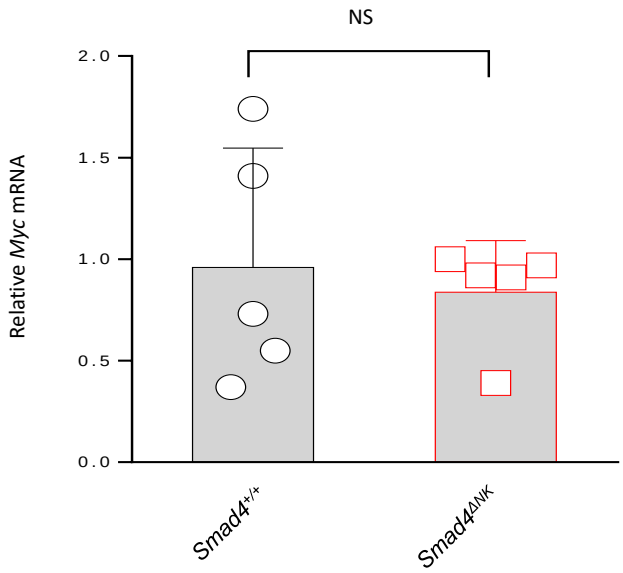

Supplemental Figure 7. Expression of *Myc* in NK cells. Expression of *Myc* in NK cells was compared between *Smad4*$^{+/+}$ and *Smad4*$^{\Delta NK}$ mice by real-time RT-PCR (n = 5). Differences were evaluated between littermates. Data are presented as mean ± SD. *P* values were calculated using paired *t* test. NS, no significance. The circles or squares on bar graphs denote data of individual mice.

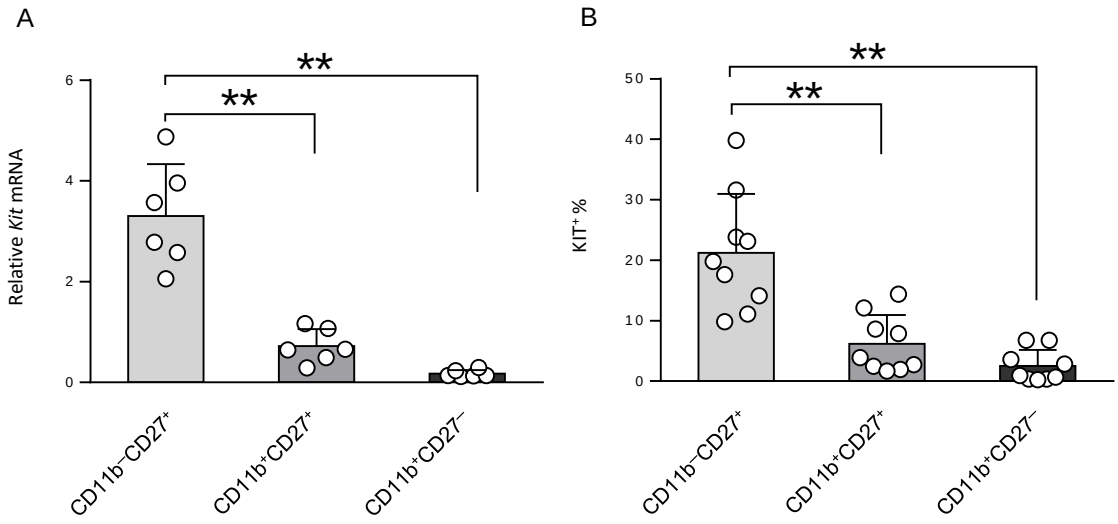

Supplemental Figure 8. Expression of *Kit* in NK cells. (**A**) Real-time RT-PCR analysis of *Kit* expression at each maturity stage of spleen NK cells (n = 6). (**B**) Flow cytometric analyses of the percentage of KIT^+ cells in spleen NK cells at each stage of maturation (n = 9). Data were represented as mean ± SD. Differences were evaluated between littermates, by one-way ANOVA and Holm's multiple comparisons test. P values were calculated using two-tailed paired t test. ** $P < 0.01$. The circles on bar graphs denote data of individual mice.

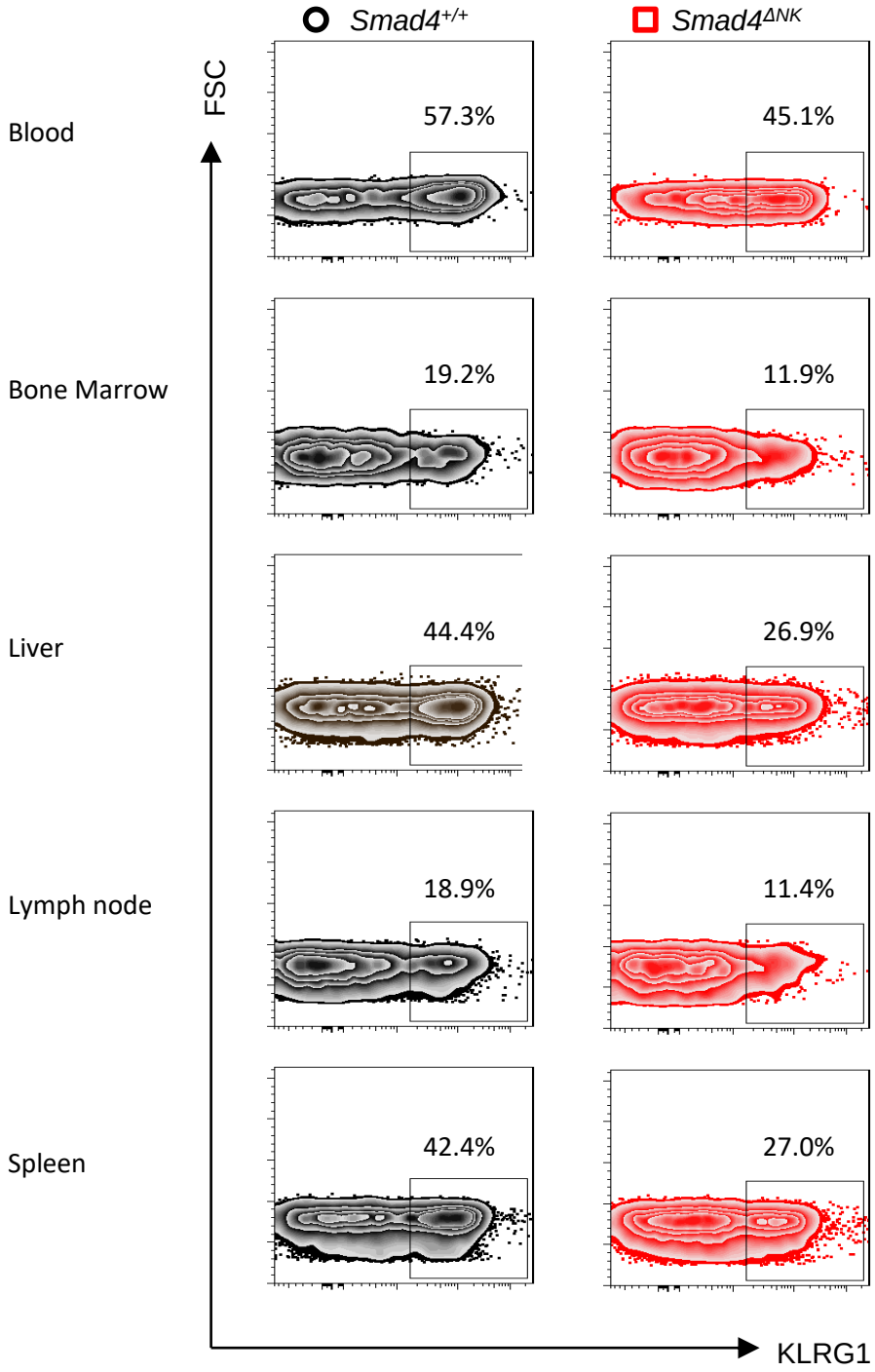

Supplemental Figure 9. Assessment of maturation of NK cells from *Smad4*$^{+/+}$ and *Smad4*$^{\Delta NK}$ mice. Representative flow cytometric analysis of the expression of KLRG1 in NK cells isolated from the blood, bone marrow, liver, lymph nodes, and spleen. Data from one of five pairs of littermate mice with similar data are presented.

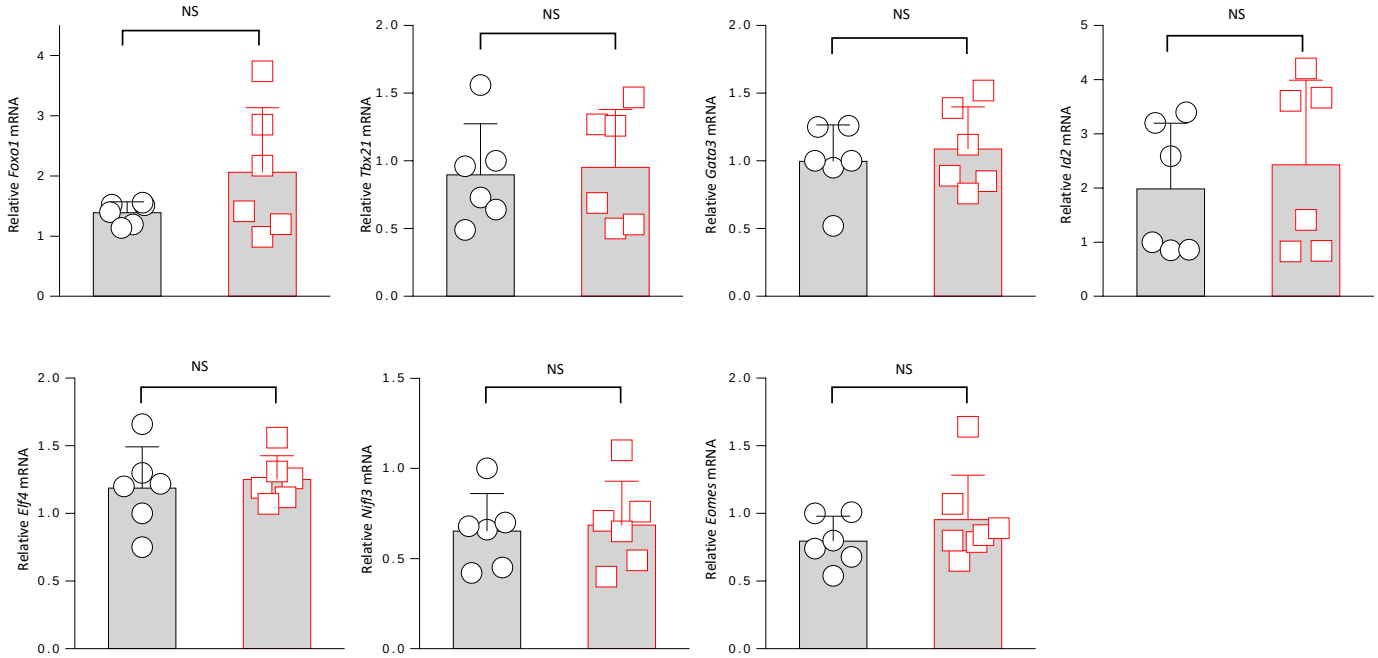

Supplemental Figure 10. Expression analysis of genes controlling NK cell terminal maturation. Expression levels of *Foxo1*, *Tbx21*, *Gata3*, *Id2*, *Elf4*, *Nifl3*, and *Eomes* in NK cells were compared between *Smad4*$^{+/+}$ and *Smad4*$^{\Delta NK}$ mice (n = 6). Differences were evaluated between littermates. Data are represented as mean ± SD. P values were calculated using two-tailed paired t test. The circles or squares on bar graphs denote data of individual mice. NS, no significance.

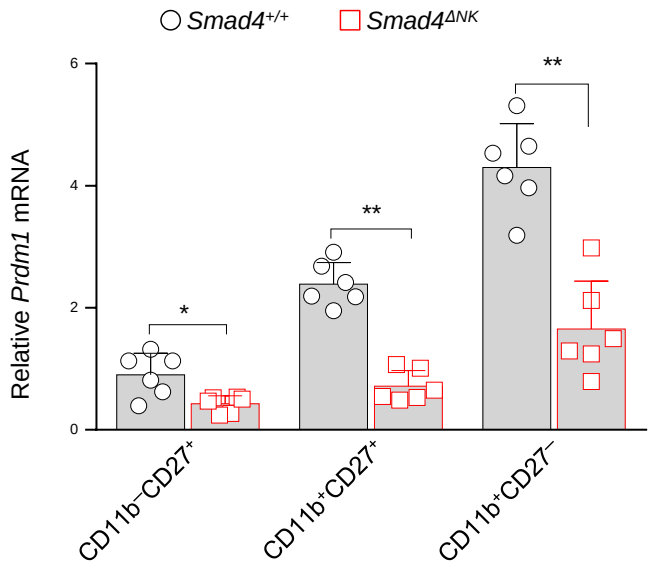

Supplemental Figure 11. Expression of *Prdm1* in NK cells at different maturation stages. Expression of *Prdm1* in NK cells at different stages of maturation was assessed by real-time RT-PCR (n = 6). Data are presented as mean ± SD. Differences were evaluated between littermates. *P* values were calculated using two-tailed paired *t* test. NS, not significant. The circles or squares on bar graphs denote data of individual mice.

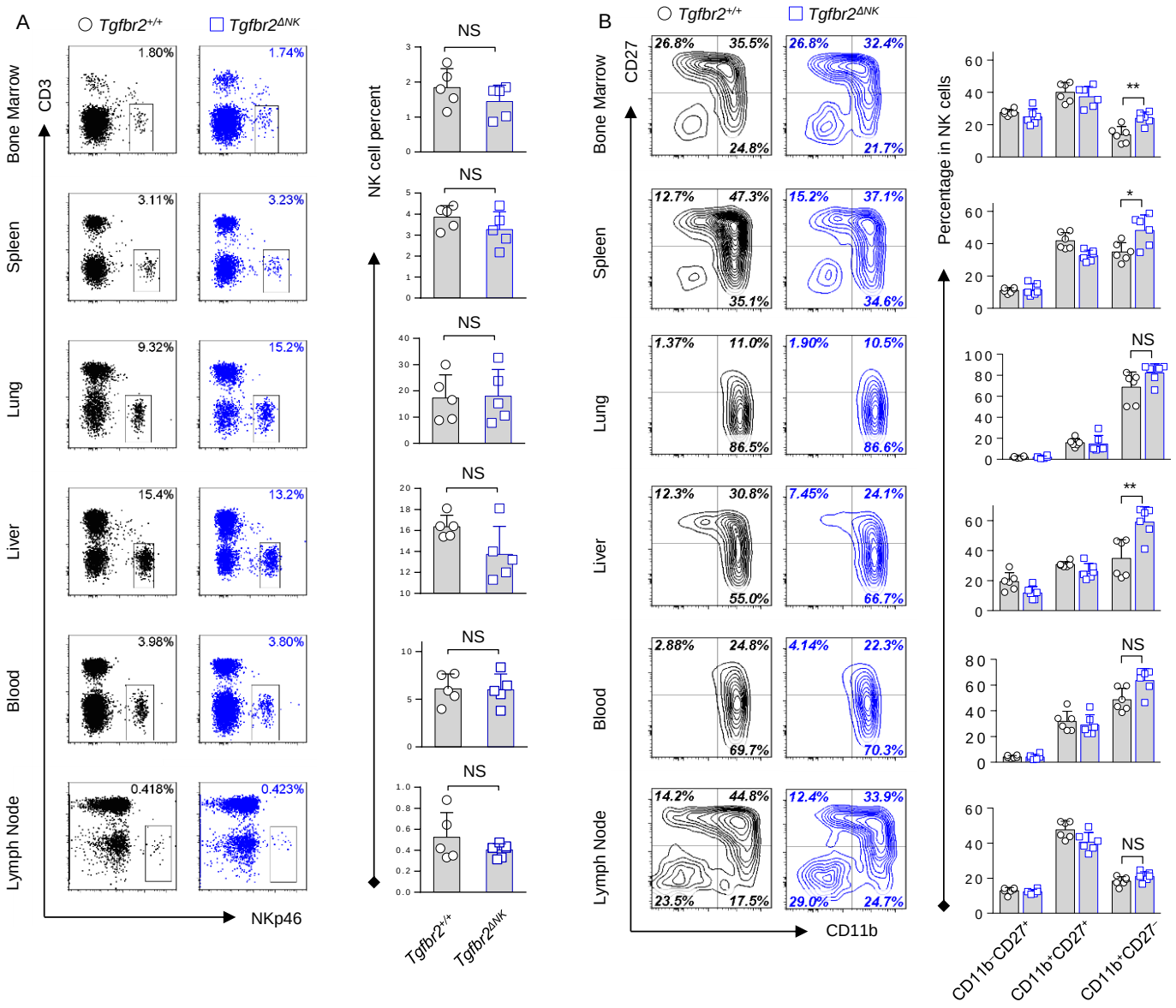

Supplemental Figure 12. Analysis of homeostasis and maturation of NK cells from *Tgfb2*$^{+/+}$ and *Tgfb2*$^{\Delta NK}$ mice. (**A**) The percentage of NK cells among lymphocytes in the bone marrow, spleen, lung, liver, blood, and lymph nodes of *Tgfb2*$^{+/+}$ and *Tgfb2*$^{\Delta NK}$ mice was determined by flow cytometry (n = 5). (**B**) Assessment of maturation status, indicated by the distribution of CD27 versus CD11b, of NK cells derived from the bone marrow, spleen, lung, liver, blood, and lymph nodes of *Tgfb2*$^{+/+}$ and *Tgfb2*$^{\Delta NK}$ mice (n = 6). Difference were evaluated between littermates. Data are represented as mean ± SD. P values were calculated using two-tailed paired t test. * $P < 0.05$ and ** $P < 0.01$. The circles or squares on bar graphs denote data of individual mice.

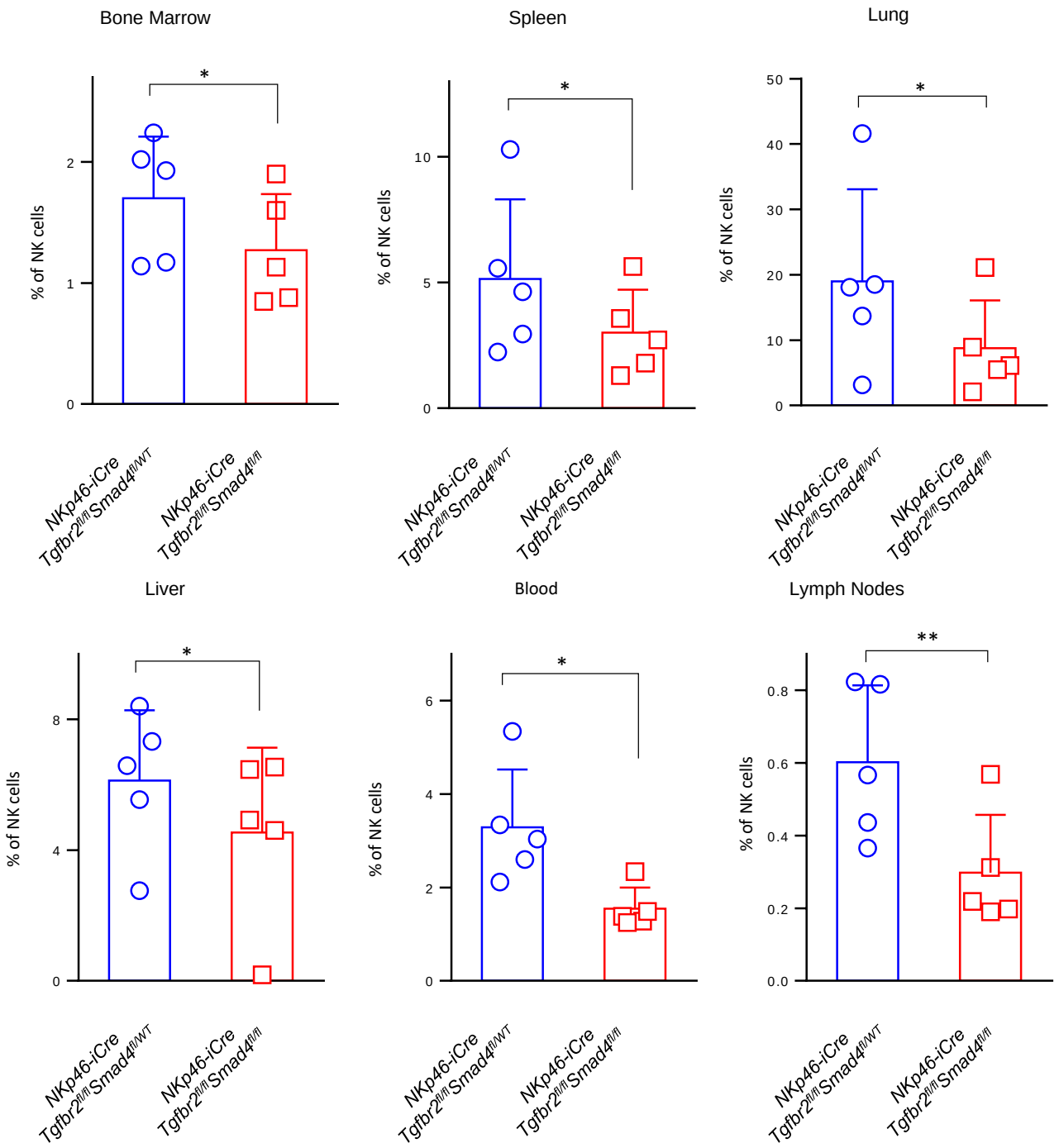

Supplemental Figure 13. Assessment of NK cell homeostasis in *Tgfbr2* and *Smad4* double knockout mice. The percentage of NK cells among lymphocytes in the indicated organs or tissues was compared between *NKp46-iCreTgfbr2*$^{fl/fl}$*Smad4*$^{fl/fl}$ and *NKp46-iCreTgfbr2*$^{fl/fl}$*Smad4*$^{fl/WT}$ mice (n = 5). Data are represented as mean ± SD. Differences were evaluated between littermates. P values were calculated using two-tailed paired t test. * $P < 0.05$ and ** $P < 0.01$. The circles or squares on bar graphs denote data of individual mice.

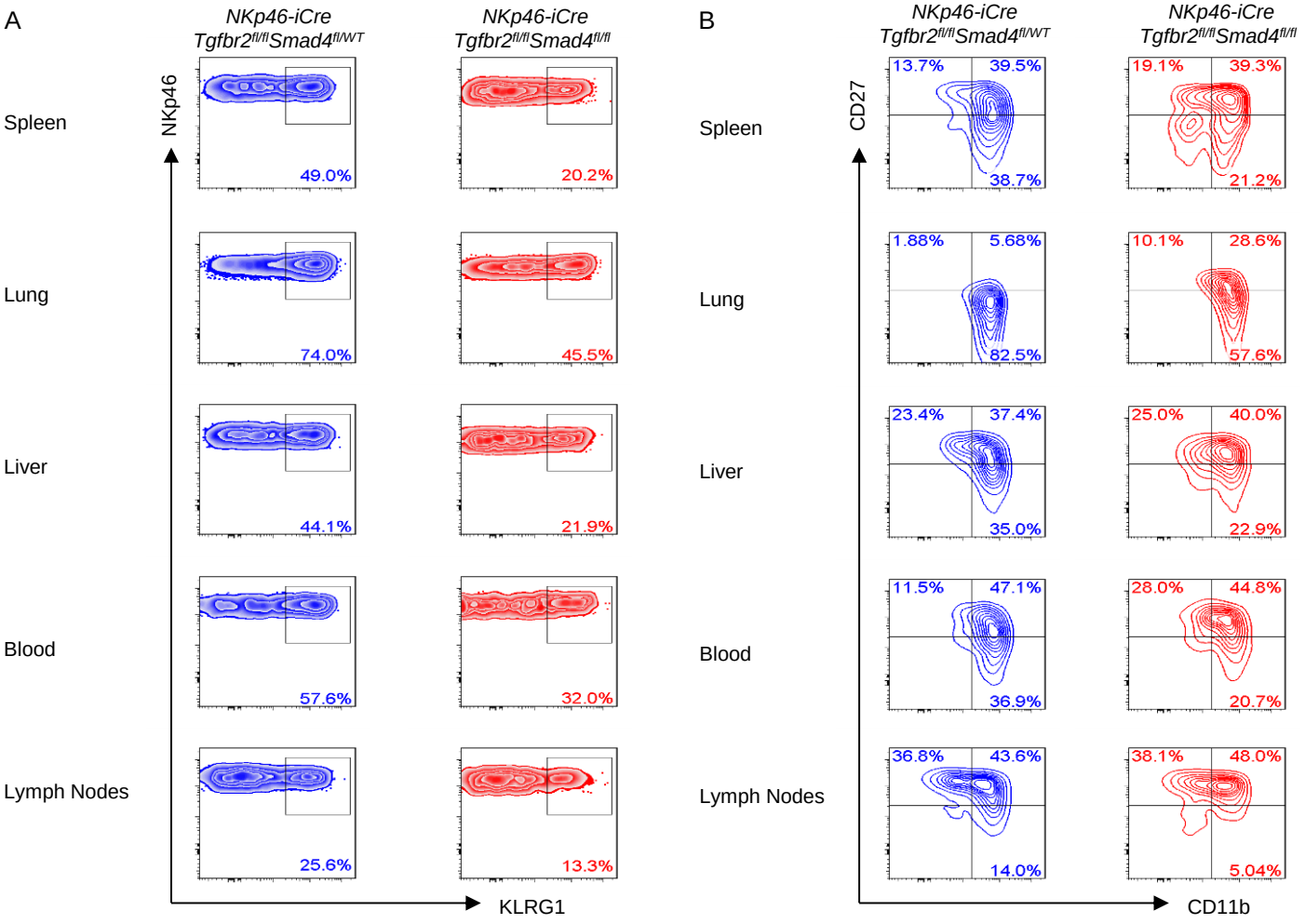

Supplemental Figure 14. Comparison of NK cell maturation in tissues of *NKp46-iCreTgfbr2$^{fl/fl}$Smad4$^{fl/fl}$* and *NKp46-iCreTgfbr2$^{fl/fl}$Smad4$^{fl/WT}$* mice. Maturation status, denoted by the expression of KLRG1 (**A**) or the distribution of CD27 versus CD11b (**B**) of NK cells derived from the spleen, lung, liver, blood, and lymph nodes was compared between *NKp46-iCreTgfbr2$^{fl/fl}$Smad4$^{fl/fl}$* and *NKp46-iCreTgfbr2$^{fl/fl}$Smad4$^{fl/WT}$* mice. Data from one of five pairs of littermate mice with similar data are presented.

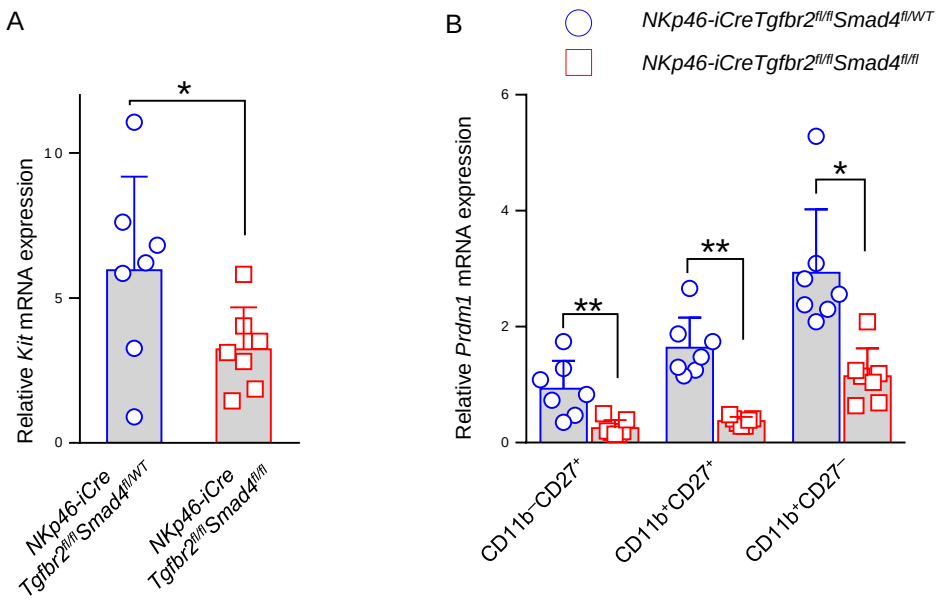

Supplemental Figure 15. Decreased expression of *Kit* and *Prdm1* in NK cells from *Tgfbr2* and *Smad4* double knockout mice. (**A**) *Kit* expression in NKp46^{+}CD3^{-}CD27^{+}CD11b^{-} splenocytes was analyzed by real-time RT-PCR. (**B**) The expression of *Prdm1* in NK cells was analyzed by real-time RT-PCR. n = 7. Data are represented as mean ± SD. Differences were evaluated between littermates. P values were calculated using two-tailed paired t test. * $P < 0.05$ and ** $P < 0.01$. The circles or squares on bar graphs denote data of individual mice.

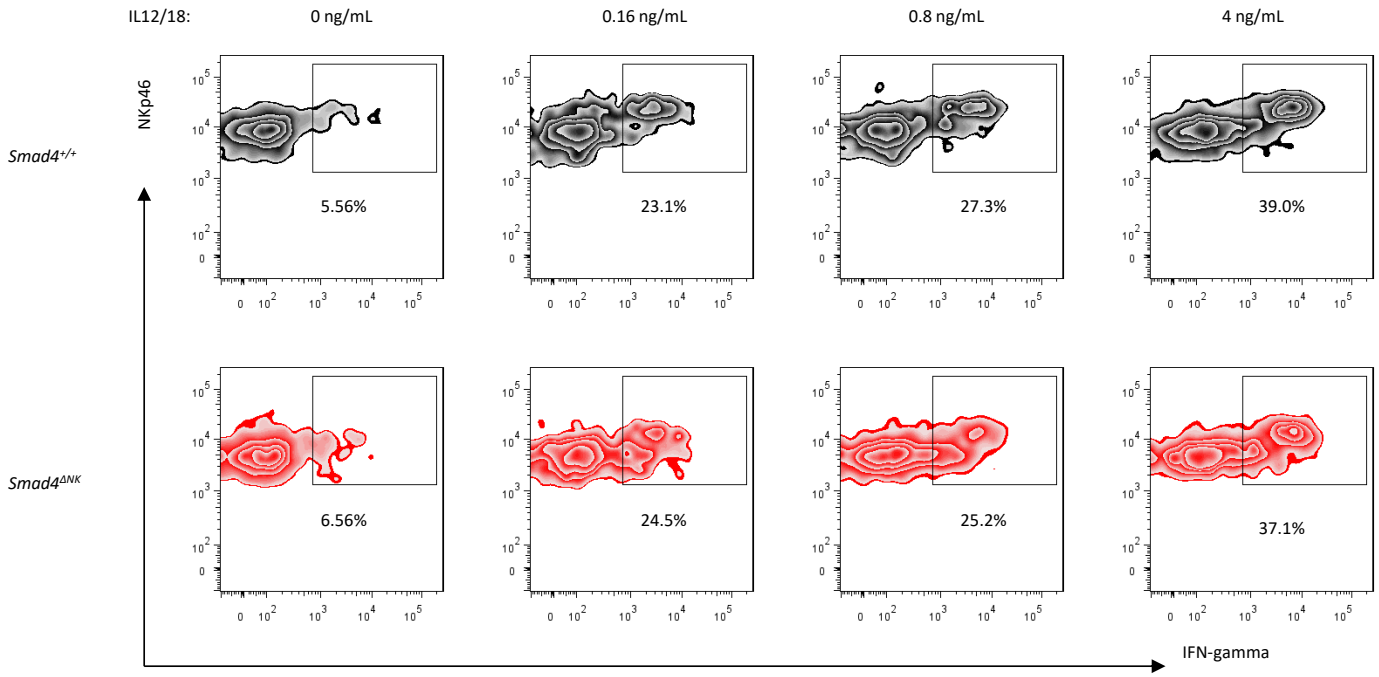

Supplemental Figure 16. *Smad4* deficiency in NK cells does not affect IFN-gamma producing capacity in the absence of TGF-β signaling. Splenocytes of *Tgfbr2*$^{\Delta NK}$*Smad4*$^{+/+}$ and *Tgfb2*$^{\Delta NK}$*Smad4*$^{\Delta NK}$ were stimulated with IL-12 plus IL-18 at the indicated concentrations for each cytokine for 24 hours, followed by intracellular flow cytometric analysis for IFN-gamma production by NKp46^{+}CD3^{-} NK cells. The experiment was repeated twice.

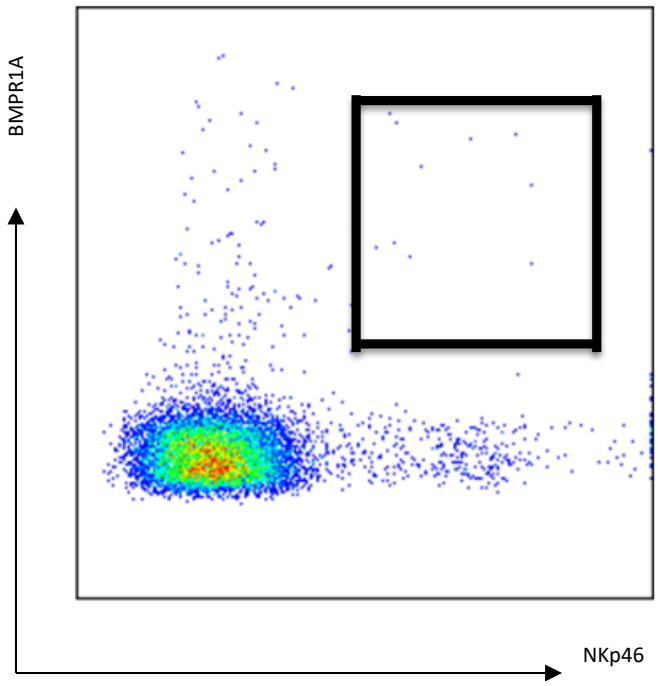

Supplemental Figure 17. Low BMP signaling in murine NK cells. The expression of BMPR1a in murine NKp46^{+}NK1.1^{+}CD3^{-} NK cells from C57BL/6 mice. The experiment was repeated twice.

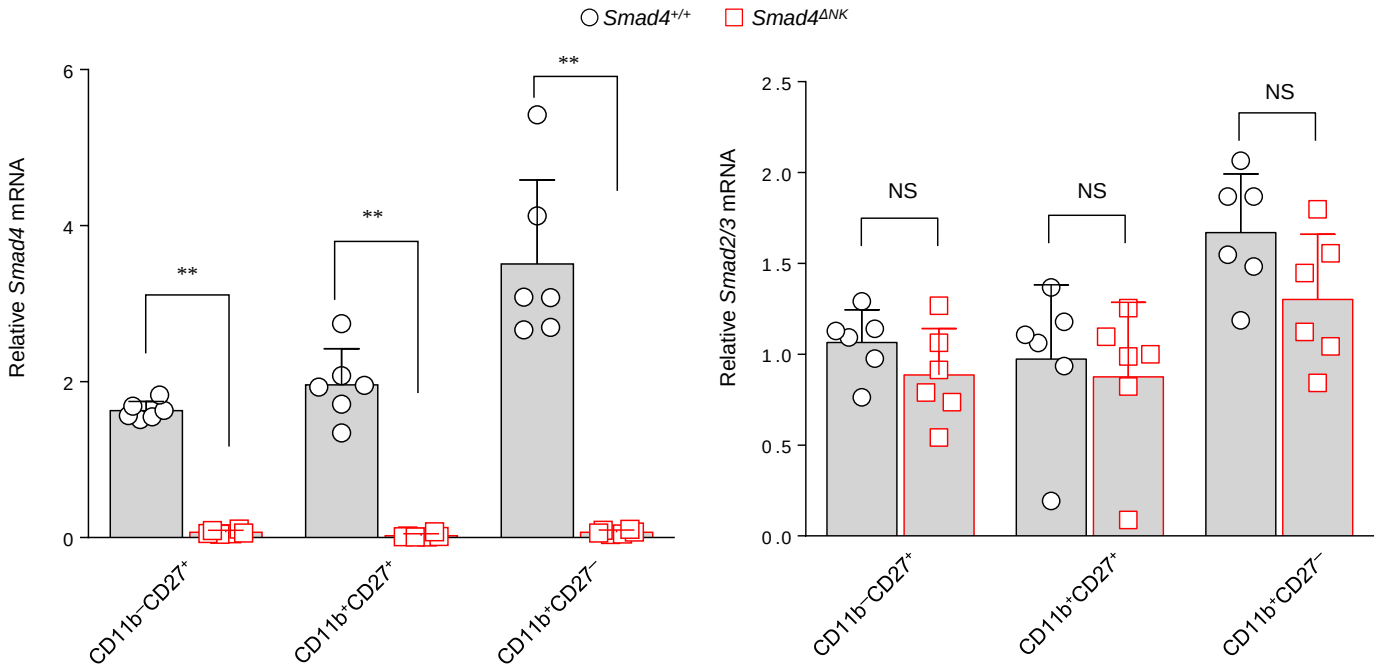

Supplemental Figure 18. Expression of *Smad2/3* in WT and Smad4-sufficient NK cells. Expression of *Smad4* and *Smad2/3* in NK cells at different stages of maturation was assessed by real-time RT-PCR (n = 6). Data are presented as mean ± SD. Differences were evaluated between littermates. *P* values were calculated using two-tailed paired *t* test. NS, not significant. The circles or squares on bar graphs denote data of individual mice.

Supplemental Table 1. Primer Sequences used for real-time RT-PCR in this study

Gene	Forward Primer	Reverse Primer 2
Elf4	CACAATGGCATCATAAGG	AGGTGGATACATCATCATC
Eomes	GGCACCAAACTGAGATGA	GGTTGAGTCCGTTTATGTTG
Foxo1	GCAATGGCTATGGTAGGATGG	TAAATGTAGCCTGCTCACTAACTC
Gata3	CTGGAGGAGGAACGCTAA	TGGATGCCTTCTTTCTTCA
Gzma	TGACTGCTGCCCACTGTAAC	TCTCCCCCATCCTGCTACTC
Gzmb	CCAAACGTGCTTCCTTTCGG	CCTGGACTCAGCTCTAGGGA
Id2	GAACACGGACATCAGCAT	GCCATTTATTTAGCCACAGAG
Junb	GGACGACCTGCACAAGATGA	TGTGGGAGGTAGCTGATGGT
Kit	CAACCAAGACAGACAAGAG	AATCATCCAGGTCCAGAG
Myc	CACCACCAGCAGCGACTC	TTGCCTCTTCTCCACAGACAC
Nifl3	GAGCAGAACCACGATAAC	AGCCTCTCATCCATCAAT
Prdm1	CAGAAACACTACTTGGTACA	GATTGCTTGTGCTGCTAA
Prf1	AGTAGAGTGTCGCATGTA	AGATGAGCCTGTGGTAAG
Smad2	AACTGTCTCCTACTACTCT	CGATTGAACACCAGAATG
Smad4	TGCATTCCAGCCTCCCATTT	CTCTCCTACCTGAACGTCCATT
Tbx21	CTACCAGAACGCAGAGAT	GACACTCGTATCAACAGATG